Journal of Basics and Applied Sciences Research (JOBASR)
ISSN (print): 3026-9091, ISSN (online): 1597-9962
Volume 4(1) January 2026
DOI: https://dx.doi.org/10.4314/jobasr.v4i1.25

Soret and Dufour Effects on Mhd Flow of Casson Fluid on A Stretching Vertical Surface in The Presence of Nonlinearized Thermal Radiation and Nth Order Chemical Reaction

Baoku, Ismail Gboyega[1*], Idris Umar[2] & Muhammad Sani[3]
[1,2]Department of Mathematics, Federal University, Dutsin-Ma, Katsina State.
[3]Department of Statistics, Federal University, Dutsin-Ma, Katsina State.
[*]Corresponding Author Email: ibaoku@fudutsinma.edu.ng

ABSTRACT
This paper investigates the heat and mass transfer characteristics of a mixed convection MHD boundary layer flow on a linearly stretching vertical surface. An incompressible Casson fluid occupying the porous space takes into account Dufour and Soret effects in the presence of nonlinearized thermal radiation, viscous dissipation, Joule heating and chemical reaction of order n. The governing partial differential equations are transformed into a set of coupled ordinary differential equations, by invoking similarity transformations. The involved nonlinear differential system is solved numerically using the Runge-Kutta-Fehlberg scheme with shooting method to determine the solutions to the velocity, temperature and species concentration profiles. Numerical values of the skin friction coefficient, Nusselt number and Sherwood numbers are also tabulated for physical interpretations of the pertinent parameters. It was established that for some kind of mixtures of light and medium molecular weight, the Soret and Dufour's effects should be taken into cognizance and increase in order of chemical reaction is confirmed to enhance Casson fluid velocity, temperature as well as concentration.

Keywords:
Casson fluid;
Natural convection;
Dufour and
Soret effects;
Stretching Surface,
nth order Chemical
Reaction.

INTRODUCTION

The study of boundary layer flow of non-Newtonian fluids has gained significant attention due to the complex nature of these fluids. Casson fluid, in particular, is an important non-Newtonian fluid that exhibits yield stress, posing challenges for modellers. Various constitutive models have been developed to elucidate the behaviour of non-Newtonian fluids, and the Casson fluid is a notable example in this regard. Ahmad *et al.* (2019) studied the heat transfer analysis for Casson fluid flow over stretching sheet with Newtonian heating and viscous dissipation. Banerjee *et al.* (2021) studied the divergent channel flow of Casson fluid and heat transfer with suction/blowing and viscous dissipation.

Additionally, the integration of thermal radiation and chemical reaction effects in boundary layer flow analysis has become increasingly important due to its practical applications. Moreover, Pal and Mondal (2011) analyzed the effects of chemical reaction on mixed convection flow of viscous fluid caused by a nonlinear stretching sheet integrated into a porous medium in the presence of thermal radiation.

Some studies focused on free convective heat transfer in a 2D- magnetohydrodynamic flow of Casson and other non-Newtonian fluids over uniform and non-uniform stretching sheets in the presence of thermal radiation and heat source/sink effects. In the same vein, Baoku *et al.* (2018) studied the influence of chemical reaction, viscous dissipation and Joule heating on MHD Maxwell fluid flow with velocity and thermal slip over a stretching sheet. Also, Kamran *et al* (2017) investigated a numerical study of magnetohydrodynamic flow in Casson nanofluid combined with Joule heating and slip boundary conditions. However, Mahanthesh *et al.* (2019) investigated quadratic convective transport of dusty Casson and dusty Carreau fluids past a stretched surface with nonlinear thermal radiation, convective condition, and non-uniform heat source or sink. The silent features of non-Newtonian fluids were considered by the Casson and Carreau fluid models. Castellanos *et al.* (2023) examined heat transfer enhancement in turbulent boundary layers with a pulsed slot jet in crossflow.

Recently, Nadeem *et al.* (2023) studied the Reynolds nanofluid model for Casson fluid flow conveying exponential nanoparticles through a slandering sheet.

How to cite this article: Baoku, I. G., Idris U. & Muhammad S. (2026). Soret and Dufour Effects on Mhd Flow of Casson Fluid on A Stretching Vertical Surface in The Presence of Nonlinearized Thermal Radiation and Nth Order Chemical Reaction. *Journal of Basics and Applied Sciences Research*, *4*(1), 227-238. https://dx.doi.org/10.4314/jobasr.v4i1.25

Jalili *et al*. (2023) investigated a nonlinear radiative heat transfer with magnetic field for non-Newtonian Casson fluid flow in a porous medium. The hybrid analytical and numerical method (HAN) were used to precisely analysed the steady flow of incompressible electrically conducting non-Darcy Newtonian Casson fluid on a vertical permeable stretchable plate with the presence of the magnetic field. Moreover, Roja *et al*. (2021) observed the irreversible investigation of Casson fluid flow in an inclined channel subject to a Darcy-Forchheimer porous medium. Prameela *et al* (2022) studied the MHD free convective non-Newtonian Casson fluid flow over an oscillating vertical plate.

Obalalu (2021) studied the heat and mass transfer in an unsteady squeezed Casson fluid flow with novel thermophysical properties. Raju *et al*. (2016) investigated heat and mass transfer in magnetohydrodynamic Casson fluid over an exponentially permeable stretching surface. Mahanta *et al* (2017) studied the hydromagnetic heat and mass transfer flow of a Casson fluid over an unsteady stretching surface with convective boundary condition. Hari and Harshad (2016) examined Soret and heat generation effects on MHD Casson fluid flow past an oscillating vertical plate embedded through porous medium, where thermal radiation and chemical reactions were considered. Reza *et al*. (2020) investigated the explicit finite difference analysis of an unsteady MHD flow of a chemically reacting Casson fluid past a stretching sheet with Brownian motion and thermophoresis effects. The impact of system parameters on skin-friction, Nusselt and Sherwood numbers were computed with discussion on streamlines and isothermal lines.

Poply *et al.* (2018) studied the stability analysis of MHD outer velocity flow on a stretching cylinder. Baoku *et al*. (2017) investigated MHD mixed convective flow of a second-grade fluid in the presence of nonlinearized thermal radiation, thermal-diffusion and diffusion-thermo effects. Khan *et al*. (2018) studied effects of heat and mass transfer on unsteady boundary layer flow of a chemically reacting Casson fluid. Animasaun (2015) analyzed the effects of thermophoresis, variable viscosity and thermal conductivity on free convective heat and mass transfer of non-Darcian MHD dissipative Casson fluid flow with suction and nth order of chemical reaction. Min *et al*. (2023) studied thermally conductive 2-D filler orientation control in polymer testing using thermophoresis.

Conclusively, Swarnalathamma *et al*. (2022) researched on combined impacts of radiation absorption and chemical reaction on MHD free convective Casson fluid flow past an infinite vertically inclined porous plate. The established equations were subsequently solved thoroughly by utilizing perturbation method. The velocity, temperature as well as concentration profiles were shown with the aids of graphs. Hussain *et al*. (2021) studied the MHD thermal boundary layer flow of a Casson fluid over a penetrable stretching wedge in the presence of nonlinear radiation and convective boundary conditions. Majeed *et al.* (2019) investigated the heat and mass transfer characteristics in MHD Casson fluid flow over a cylinder in a wavy channel using higher-order FEM computations.

However, none of the above literature considers the combinations of governing parameters such as nonlinearized thermal radiation, Joule heating with viscous dissipation, heat generation/absorption, nth order chemical reaction involving Soret and Dufour effects on MHD boundary layer flow of a chemically reactive non-Newtonian Casson fluid, as applicable in biomedical engineering (blood flow with hyperthermia) and polymer processing (electrically heated extrusion), as being considered in this research.

MATERIALS AND METHODS

Mathematical Formulation for Model

A steady laminar boundary layer mixed convective flow, heat and mass transfer of a non-Newtonian Casson fluid in the presence of nonlinearized thermal radiation, heat absorption/generation and nth order chemical reaction is considered in a porous medium. Assuming the rheology of a two-dimensional hydromagnetic flow of Casson fluid with Soret and Dufour effects over a heated linear vertical stretching surface which coincides with the plane ($y = 0$) is subjected to a transverse magnetic field of strength B_o. The flow is restricted to the zone ($y > 0$) as displayed in Figure 1. Two adjacent forces are pressured to the exerted towards the y-axis, which allow the stretching of the sheet. The surface permeability properties are engendered in order to analyze the suction and blowing processes, while viscous and Joules dissipations are incorporated. The dynamical equations for an isotopic rheology of Casson fluid under consideration can be represented as:

$$\tau_{ij} = \begin{Bmatrix} 2(\mu_B + P_y/(2\pi)^{1/2})e_{ij}, & \pi > \pi_c \\ 2(\mu_B + P_y/(2\pi)^{1/2})e_{ij}, & \pi < \pi_c \end{Bmatrix}$$

where $\pi = e_{ij}e_{ij}$ and e_{ij} are $(i,j)^{th}$ component of the deformation rate, π is the product of the component of the deformation rate with itself, π_c is the critical value of their product based on the non-Newtonian model, μ_j represents the plastic dynamic viscosity of the non-Newtonian fluid P_y is the yield stress of the fluid.

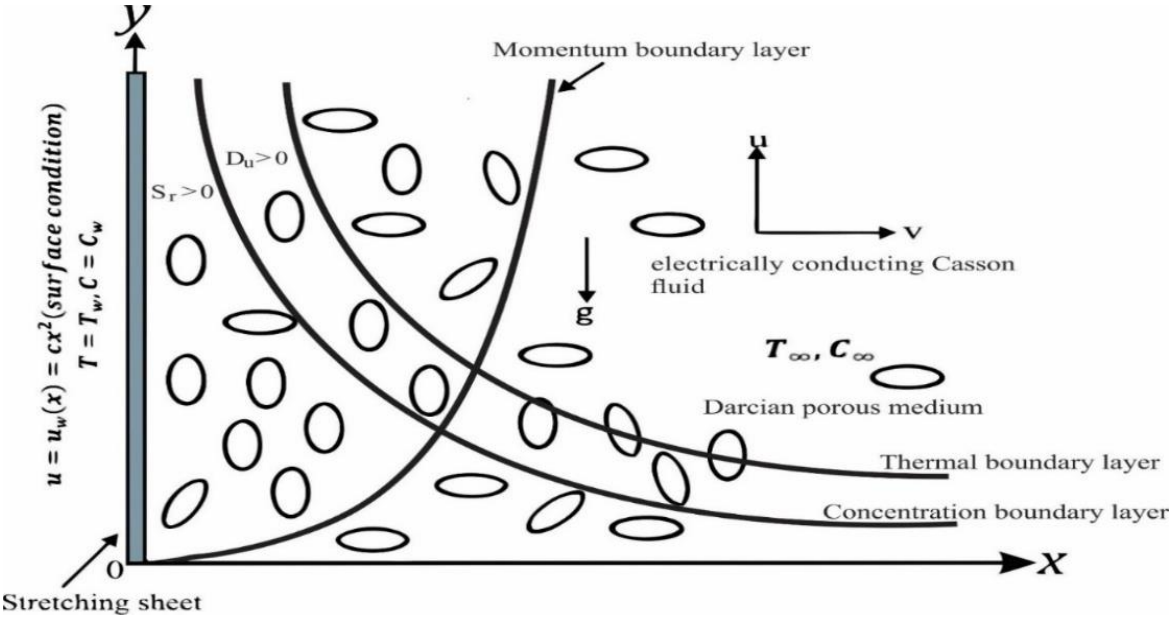

Fig. 1: Schematic diagram of the physical model and coordinate system

The following are the governing equations for the model:

$$\frac{\partial u}{\partial x} + \frac{\partial v}{\partial y} = 0 \quad (1)$$

$$u\frac{\partial u}{\partial x} + v\frac{\partial u}{\partial y} = v\left(1+\frac{1}{\beta}\right)\frac{\partial^2 u}{\partial y^2} - \left(\frac{v}{K} + \frac{\sigma {B_0}^2}{\rho}\right)u + g\beta_T(T-T_\infty) + g\beta_c(C-C_\infty) \quad (2)$$

$$u\frac{\partial T}{\partial x} + v\frac{\partial T}{\partial y} = \alpha\left(\frac{\partial^2 T}{\partial y^2} - \frac{1}{\kappa}\frac{\partial q_r}{\partial y}\right) + \frac{K_T D_m}{C_s C_p}\frac{\partial^2 C}{\partial y^2} + \left(\frac{\mu}{\rho C_p} - \frac{1}{\beta}\right)\left(\frac{\partial u}{\partial y}\right)^2 + \frac{1}{\rho C_p}\sigma B_0^2 u^2 \quad (3)$$

$$u\frac{\partial C}{\partial x} + v\frac{\partial C}{\partial y} = D_m\frac{\partial^2 c}{\partial y^2} + \frac{D_m K_T}{T_m}\frac{\partial^2 T}{\partial y^2} - Kr(C-C_\infty)^n \quad (4)$$

with boundary conditions:

$$u = u_w(x) = ax,\ v = -v(x),\quad T = T_w,\ C = C_w \quad \text{at } y = 0 \quad (5)$$

$$u \to 0,\quad C \to C_\infty,\quad T \to T_\infty,\quad as\quad y \to \infty \quad (6)$$

where u, v are the velocity components, κ is thermal conductivity, α is the thermal diffusivity, υ is the kinematic viscosity, ρ is the density of the fluid, β is the Casson fluid parameter, D_m is the mass diffusivity, C_s is the heat capacity, C_p is the specific heat at constant pressure; σ is the electrical conductivity of the fluid; K_T, T_m are the thermal diffusion ratio, mean fluid temperature respectively, q_r is the radiative heat flux, Kr is the rate of chemical reaction.

Using similarity variables;

$$\eta = y\sqrt{\frac{a}{v}},\ \psi = x\sqrt{av}\ f'(\eta),\ \theta(\eta) = \frac{T-T_m}{T_\infty - T_m}, \phi(\eta) = \frac{C-C_\infty}{C_w - C_\infty} \quad (7)$$

where ψ is the stream function, the velocity components are defined as:

$$u = \frac{\partial \psi}{\partial y},\quad v = -\frac{\partial \psi}{\partial x} \quad (8)$$

and consequently;

$$u = ax'(\eta),\ v = -\sqrt{av}\ f(\eta) \quad (9)$$

Using similarity variable, we obtained the following dimensionless system of ordinary differential equations;

$$\left(1+\frac{1}{\beta}\right)f''' + f'f'' - f'^2 - (P+M)f' + \lambda(\theta + N\phi) = 0 \quad (10)$$

$$[1 + PrR(\theta + Cr)^3]\theta'' + Prf\theta' + 3PrR(\theta + Cr)^2\theta'^2 + +DuPr\phi'' + Br(1+\beta)f''^2 + MBrf'^2 - PrH\theta = 0 \quad (11)$$

$$\phi'' + SrSc\theta'' + Scf\phi - KrSc\phi^n = 0 \quad (12)$$

with the following boundary conditions:

$$f(0) = s,\quad f'(0) = 1,\quad f'(1) = 0,\quad \theta(0) = 1,\ \phi(0) = 1\ at\ \eta = 0 \quad (13)$$

$$f'(\infty) \to 0,\quad \theta(\infty) \to 0,\quad \phi(\infty) \to 0 \quad \text{as } \eta \to \infty \quad (14)$$

where $s = \frac{v_0}{\sqrt{\frac{U_0 v}{2L}}}$, s is the suction for $s > 0$ and $s < 0$ for injection, $P = \frac{v}{K_a}$ is the porous medium parameter,

$M = \frac{\sigma\beta_0^2}{\rho_a}$ is the magnetic field parameter, $\lambda = \frac{G_{r_x}}{Re_x^2}$ is the mixed convection parameter, $N = \frac{Bc(C_\omega - C_\infty)}{B_T(T_\omega - T_\infty)}$ is the natural convection parameter, $Pr = \frac{K\upsilon}{\rho C\rho}$ is the Prandtl number, $Du = \frac{K_\tau D_m(C_\omega - C_\infty)}{C_s C_\rho \upsilon(T_\omega - T_\infty)}$ is the Dufour number, $Br = \frac{\mu \cup^2}{\kappa(T_w - T_\infty)}$ is the Brickman number, $Sc = \frac{\nu}{D_m}$ is the Schmidt number and $Sr = \frac{K_\tau D_m(T_\omega - T_\infty)}{\tau_m \upsilon(C_\omega - C_\infty)}$ is the Soret number, $Cr = \frac{T_\infty}{T_w - T_\infty}$ is the temperature difference, $R = \frac{4\sigma * T_\infty^3}{K^* K}$ is the thermal radiation parameter, H is the heat source/sink, Kr is the rate of chemical reaction, n is the order of chemical reaction.

The quantities of physical interest are the coefficient of skin-friction, Nusselt and Sherwood numbers which are respectively defined as:

$$C_f = \frac{\tau_w}{\frac{1}{2}\rho_w^2},\ Nu_x = \frac{xq_w}{K(T_w - T_\infty)},\ Sh_x = \frac{xJ_w}{D_m(C_w - C_\infty)}$$

where $T_w = \left[-\mu[1+\beta]\frac{\partial u}{\partial y}\right]_{y=0}$, $q_w = -K\left(\frac{\partial \tau}{\partial y}\right)_{y=0}$, $J_w = -D_m\left(\frac{\partial x}{\partial y}\right)_{y=0}$ and consequently:

$\frac{1}{2}C_f Re^{1/2} = \left(1 + \frac{1}{\beta}\right)f''(0)$; $Re^{1/2}Nu_x = -\theta'(0)$; and $Re^{1/2}\,Sh_x = -\phi(0)$;

where $Re = \frac{x\mu_w}{\upsilon}$ is Reynolds number.

Numerical Method of the Solution

Physics of the problems in every fields of engineering sciences do lead to set of linear or nonlinear differential equations as its governing equations. In accordance with the physics of this problem and its obtained mathematical formulation, sufficient boundary conditions are available in order to achieve solutions to the problem under consideration. The nonlinear differential equations (10)–(12) along with the boundary conditions (13) and (14) are solved using Runge-Kutta-Fehlberg (RKF) integration scheme with shooting method, by converting them into initial value problem (IVP). The most important part of this scheme is to determine the appropriate finite value of η_∞ which is estimated by starting with some initial guess value and solve the resulting initial value problem consisting of equations of the model to find the proper value of $f''(0)$, $\theta'(0)$, and $\phi'(0)$. This process is repeated again by considering another large value of η_∞ until two successive value of $f''(0)$, $\theta'(0)$, and $\phi'(0)$ are obtained up to a desired significant digit. Consequently, the final value of $\eta \to \infty$ is obtained for a particular set of physical parameters for determining velocity $f'(\eta)$, temperature $\theta(\eta)$ and concentration $\phi(\eta)$ in the boundary layer.

Once all the seven initial conditions for the IVP are known, then we can proceed to solve the system of simultaneous solutions by using the RKF method with the shooting technique. The value of $\eta \to \infty$ is selected to vary depending upon a set of physical parameters in order to avoid numerical oscillations. The solutions are finalized by adjusting the initial guess based on the residual using Newton's method to refine the initial guess to shoot towards the better ends of the boundary condition as given. The solution codes for Nusselt number as described above are validated with the numerical results available in the literature under some limiting cases:

Table 1: Validation of the values of $\theta'(0)$ for thermal radiation parameter R, Magnetic parameter M and Prandtl number Pr for Casson fluid with those of Prakash *et al.* (2016)

R	M	Pr	Prakash *et al.* (2016)	Present results
0	0	1	-0.954813	-0.95481061118855
0	0	2	-1.471457	-1.47145401612198
0	0	3	-1.869071	-1.86906879948559
0	0	5	-2.500119	-2.50012796085512
0	0	10	-3.660360	-3.66036932692199
1	0	1	-0.861508	-0.86150863461719
0	1	1	-0.535302	-0.53530117279701
1	1	1	-0.461966	-0.46196546193784

Translating the algorithm of RKF with shooting technique into Maple codes for several sets of emerging parameters and the set of systems of boundary value problems obtained from Equations (10) – (14), the step size of □□□□□0.001 is set for the computational purposes and the error tolerance of 10^{-5} is used in all the cases during coding as described by Herck (2003) to obtain the results. Hence, the solutions, of the resulting coupled highly nonlinear equations (10) - (12) which are higher order boundary value problems alongside the conditions (13) - (14), are available.

RESULTS AND DISCUSSION

A numerical analysis is carried out to examine how different thermophysical parameters affect the flow, heat, and mass transfer characteristics of Casson fluid. The impacts of these physical parameters on velocity,

temperature and concentration profiles are discussed and illustrated graphically in the figures below:

Velocity Profiles

Figure 2 represents the effect of Casson fluid parameter β on velocity profile f', where the result shows that an increase in the Casson fluid parameter leads to decrease in the velocity profile. Figure 3 shows the effect of porous medium parameter P on the velocity profile f', where the result shows an increase in the porous medium lead to decrease in the velocity profile. Figure 4 represents the effects of suction parameter s on velocity profile f', where the result shows that as the suction increases, the velocity profile shifts downward, meaning the fluid velocity decays more quickly. The changes are significant, showing that increasing s leads to a lower velocity profile

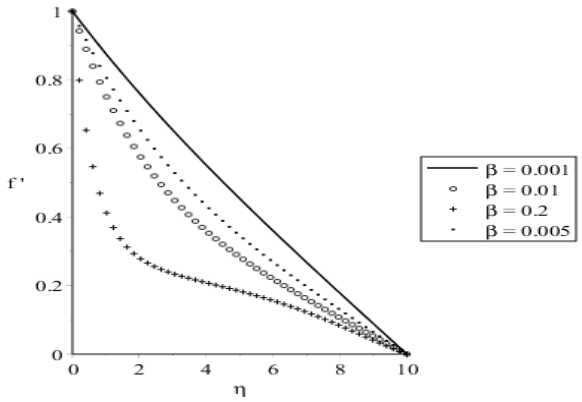

Figure 2: Velocity profile f'or different values of Casson fluid parameter β.

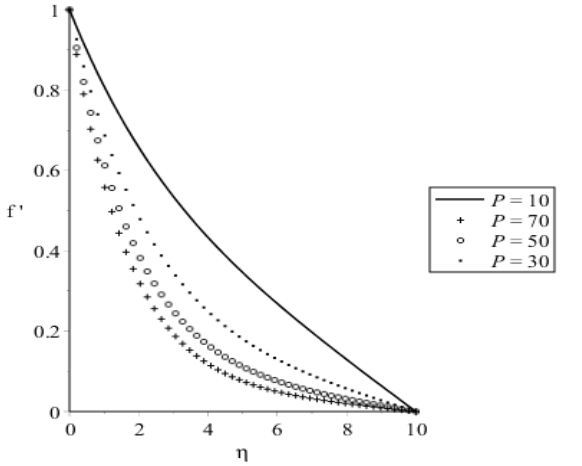

Figure 3: Velocity profile f' for different values of porous medium parameter P.

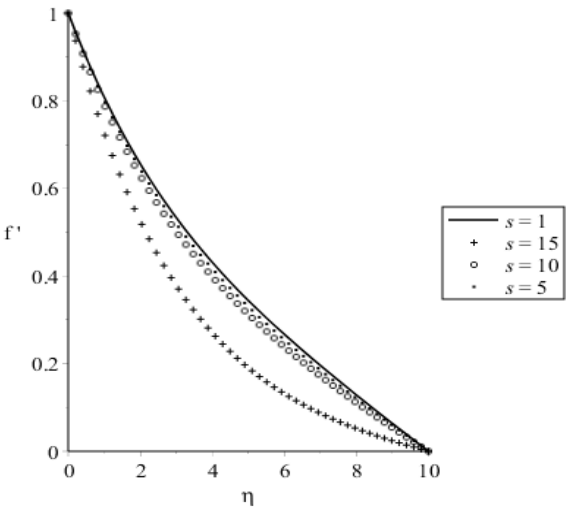

Figure 4: Velocity profile f for different values of suction parameter s.

Figure 5 depicts the effect of magnetic field parameter M on velocity profile f'. It is noted that an increase in the magnetic field parameter leads to a decrease in the velocity profile. Figure 6 depicts the effect of mixed convection on velocity profile λ. It shows that as the mixed parameter increase, the velocity profile f'retains higher values.

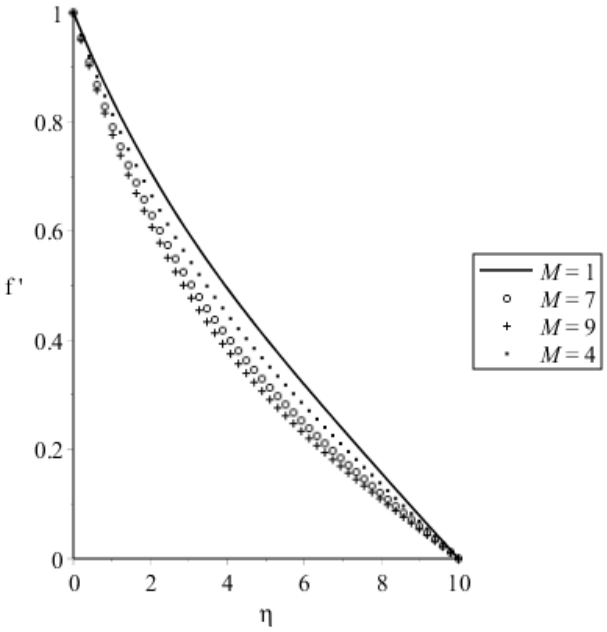

Figure 5: Velocity profile $f'$for different values of magnetic field parameter M.

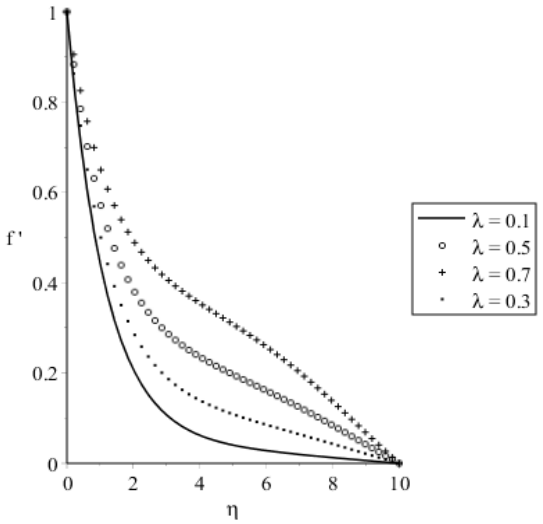

Figure 6: Velocity profile f' for different values of Mixed convection parameter λ.

Temperature Profiles

Figure 7 displays the effect of Casson fluid parameter β on temperature profile θ. It is discovered that an increase in the Casson fluid parameter β leads to an increase in the temperature profile θ. Figure 8 depicts the effect of Dufour number Du on temperature profile θ. It noted that as Dufour Du increases, the temperature profile θ reduces, showing a significant impact of thermal diffusion. A higher Du number means that mass diffusion reduces thermal energy transport, lowering the temperature in the system.

Figure 9 represent the effect of thermal radiation parameter R on temperature profile θ. It is observed that an increasing radiation parameter leads to increasing temperature. A higher R means more thermal radiation is present and thereby, leading to higher energy retention in the system. Lower R values indicate a faster decay in θ, meaning stronger heat loss due to thermal radiation. Figure 10 represents the effect of heat source parameter H on temperature profile. The results show that an increase in the heat source leads to decrease in the temperature profile. As H increases from 10 to 50, it contributes to higher internal volumetric heat generation in the system.

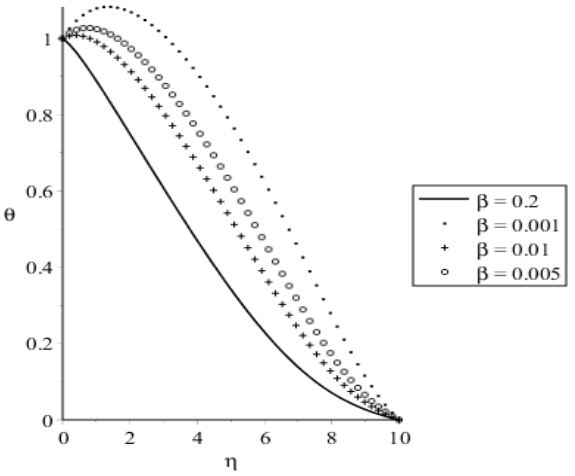

Figure 7: Temperature profile θ for different values of Casson parameter β.

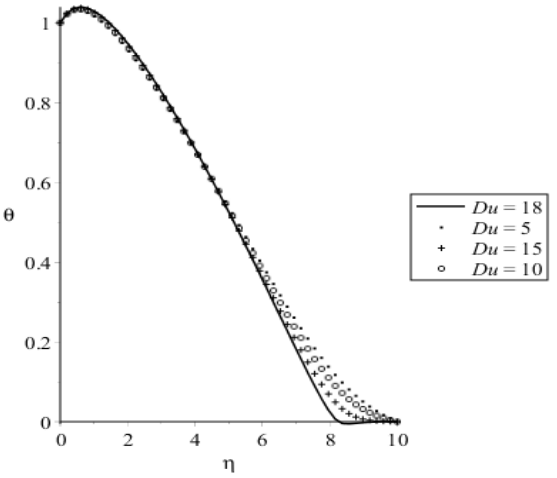

Figure 8: Temperature profile θ for different values of Dufour number Du.

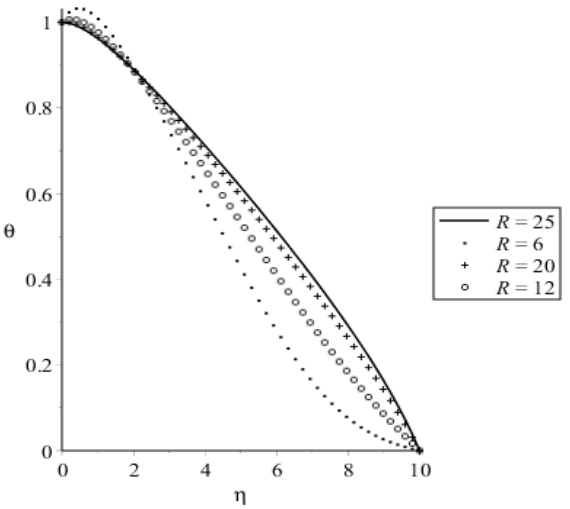

Figure 9: Temperature profile θ for different values of radiation parameter R.

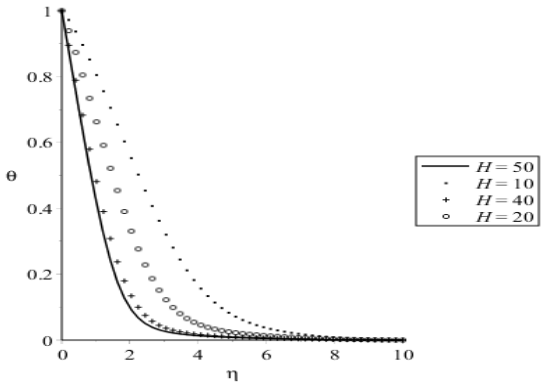

Figure 10: Temperature profile θ for different values of heat source parameter H.

Figure 11 represents the effect of suction parameter s on temperature profile θ. It is noted that an increase in the suction parameter leads to a decrease in the temperature profile more significantly especially when the suction parameter is greater than 5. Figure 12 represents the effect of porous medium parameter P on temperature profile θ. The results show an increase in porous medium leads to decreases more rapidly in temperature. Figure 13 features the effect of Brinkman number Br on temperature profile θ. It is observed that the higher Br enhances temperature. This confirms that the frictional force from fluid viscosity significantly heats the Casson fluid.

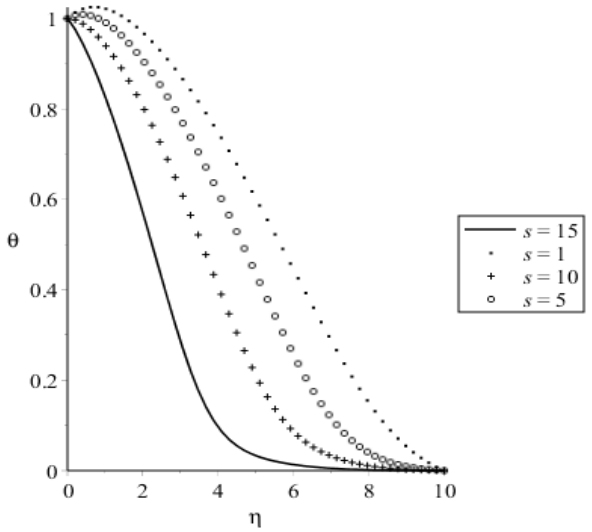

Figure 11: Temperature profile θ for different values of Suction parameter s.

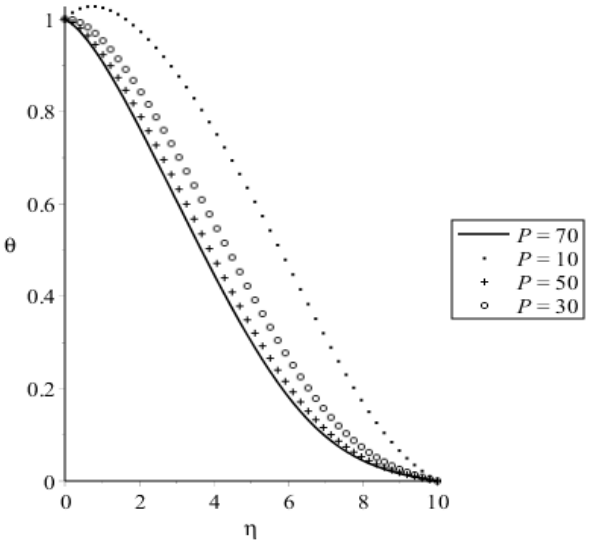

Figure 12: Temperature profile θ for different values of porous medium parameter P.

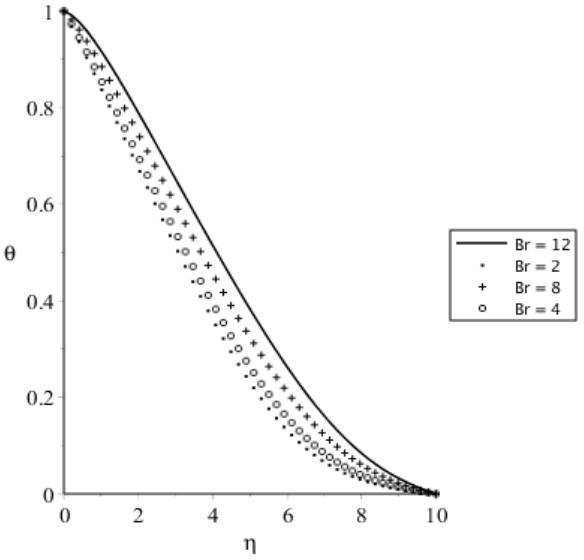

Figure 13: Temperature profile θ for different values of Brinkman parameter Br.

Concentration Profiles

Figure 14 represents the effect of Casson parameter β on concentration. The results reveal that as the Casson parameter increases, it leads to decrease in concentration profile. As β increases, the function ϕ decreases more rapidly, indicating a stronger attenuation effect. Figure 15 shows the effect of magnetic field parameter on concentration profile. It discovered that increase M decrease concentration profile, Higher M values shift the curve downward more significantly. Figure 16 depicts the effect of porous medium parameter P on concentration profile. The results show when the porous medium

increases, it leads to rapid decrease in concentration profile.

Figure 17 examines the effect of Schmidt number Sc on concentration profile. It shows that as Sc increases, the concentration ϕ increases away from the boundary layer along η. This implies that the momentum diffusivity overcomes mass diffusivity or thinner concentration boundary layer (away from the wall) as there exists a weak molecular wall concentration or generation at the surface. Figure 18 displays the effect of chemical reaction parameter Kr on the concentration profile. It is observed that an increasing in Kr results into a significant reduction on ϕ, meaning that the concentration decreases more rapidly as η increases. A higher Kr value implies stronger chemical reactions that enhance the consumption of species, leading to lower concentration profiles.

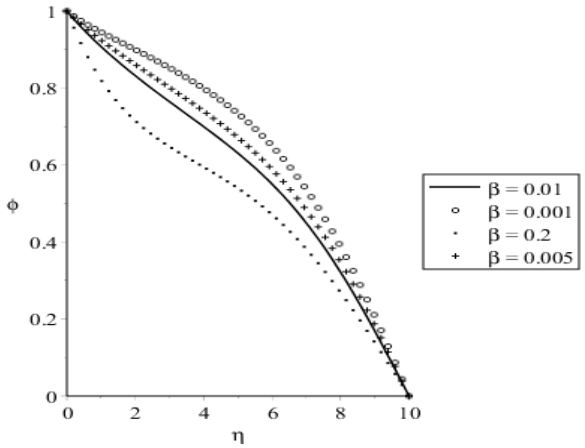

Figure 14 Concentration profile ϕ for different values of Casson parameter β.

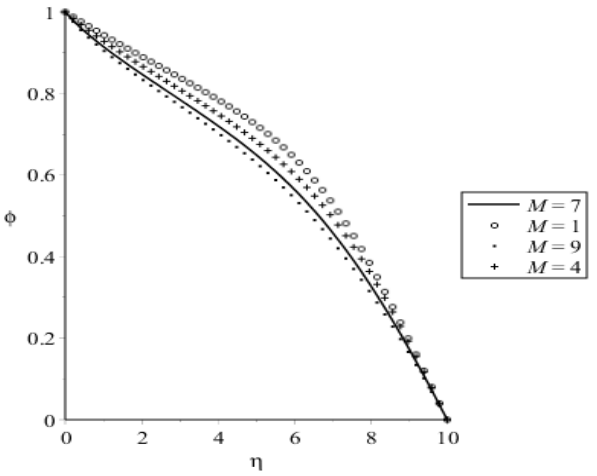

Figure 15: Concentration Profile ϕ for different values of Magnetic Field parameter M.

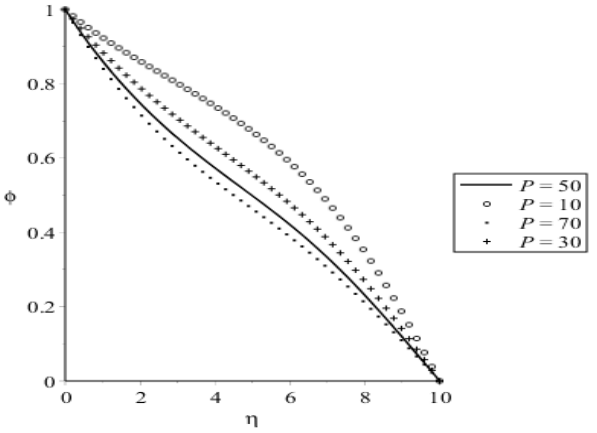

Figure 16: Concentration Profile ϕ for different values of Porous Medium parameter P.

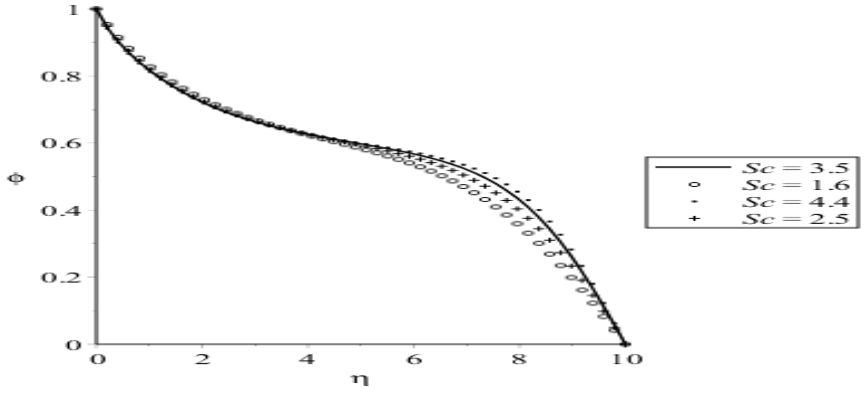

Figure 17: Concentration Profile ϕ for different values of Schmidt number Sc.

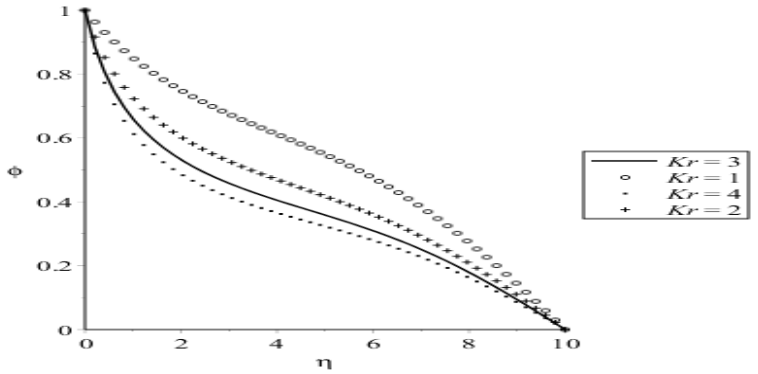

Figure 18: Concentration profile ϕ for different values of chemical reaction parameter Kr.

Table 2: Numerical Values for Skin-friction Coefficient, Nusselt and Sherwood Numbers for Casson, Magnetic Field and Mixed Convection Parameters with Prandtl and Schmidt Numbers.

B	M	Pr	Sc	N	$-f''(0)$	$-\theta'(0)$	$-\phi'(0)$
0.001	5	5	0.62	10	0.128841011704353	0.0701839860095256	0.144190884273840
0.01					0.291654789032826	0.107773712702325	0.045922101357412
0.1					0.854572623312616	0.19376930025114	-0.04808517658152
0.001	5	5	0.62	10	0.128841011704353	0.0701839860095256	-0.04808517658152
	6				0.131663670080814	0.079622843670195	0.210155684445088
	7				0.134466109737242	0.0897549737364017	0.275894054951321
0.001	5	5	0.62	10	0.128841011704353	0.0701839860095256	0.144190884273840
		10			0.128840547507094	0.0702369851385807	0.144568367062427
		15			0.128840392317485	0.0702547021266235	0.144694461115706
0.001	5	5	0.62	10	0.128841011704353	0.0701839860095256	0.144190884273840
			1.24		0.128598205942026	0.0839805246813650	0.144695100016448
			1.86		0.133095721783517	0.0962819757474453	0.136623397229302
0.001	5	5	0.62	10	0.128841011704353	0.0701839860095256	0.144190884273840
				20	0.110246556786514	0.0656668338422958	0.164705220774951
				30	0.091113122728759	0.0613295481967239	0.187554834450779

Table 3: Numerical Values for Skin-friction Coefficient, Nusselt and Sherwood Numbers for Porous Medium, Suction and Chemical Reaction Parameters with Dufour and Soret Numbers

Du	P	s	Sr	Kr	$-f''(0)$	$-\theta'(0)$	$-\phi'(0)$
0.2	10	0.5	0.5	1	0.128841011704353	0.0701839860095256	0.144190884273840
0.4					-0.12884123106245	0.0702002618575509	0.144153897814206
0.6					0.128841448947599	0.0702165768793141	0.144117084822046
0.2	10	0.5	0.5	1	0.128841011704353	0.0701839860095256	0.144190884273840
	15				0.143021025709591	0.0735987252194601	0.131066027615618
	20				0.156484232856710	0.0769171108003090	0.119387040815415
0.2	10	0.5	0.5	1	0.128841011704353	0.0701839860095256	0.144190884273840
		1			0.129087893429945	0.0703340733343109	0.142235856456812
		1.5			0.129335813034116	0.0704763730524983	0.140139481086111
0.2	10	0.5	0.5	1	0.128841011704353	0.0701839860095256	0.144190884273840
			1		0.129016226198021	0.0971603193601236	0.144105521717104
			1.5		0.129199876541646	0.1245860292262900	0.144011660565614

0.2	10	0.5	0.5	1	0.128841011704353	0.0701839860095256	0.144190884273840
				2	0.131956716398227	0.3843587711973350	0.141515799606986
				3	0.133516459249944	0.5939981689123100	0.140421263589198

CONCLUSION

The research examines heat and mass transfer of a hydromagnetic boundary layer Casson fluid in a porous medium; considering Soret and Dufour effects in the presence of nonlinearized thermal radiation, n[th] chemical reaction, Joule heating and viscous dissipation. The research describes phenomena as being experienced in blood flow with hyperthermia and in electrically heated extrusion. After non-dimensionalization of the boundary layer equations for the model, the resulting highly nonlinear system of ordinary differential equations are solved numerically using the fifth-order Runge-Kutta-Fehlberg integration scheme with shooting method.

The effects of various significant parameters on the dimensionless velocity, temperature and species concentration profiles are shown graphically. The study successfully demonstrates that thermophysical effects significantly impact the heat and mass transfer characteristics of Casson fluid. Increased Casson fluid viscosity enhances resistance to fluid motion, reducing the rate of heat and mass transfer. Thermal radiation and rate of chemical reaction parameters play crucial roles in temperature and concentration profiles, respectively. The research provides a deeper understanding of fluid dynamics in complex systems, with practical implications in fields such as biomedical engineering, food processing, and polymer industries.

Nomenclature

Alphabetical Symbol

B_o Magnetic strength intensity
Br Brinkman number
C Concentration
C_f Skin friction coefficient
C_p Specific heat at constant pressure
Cr Temperature difference parameter
C_s Concentration susceptibility
C_w Concentration at the wall/plate
C_∞ Free steam concentration
D_m Coefficient of mass diffusivity
Du Dufour number
f Dimensionless velocity
Gr_x Grashof number
g Acceleration due to gravity
H Heat generation/absorption parameter
I Identity tensor
i, j Horizontal and vertical component of u and v
K Permeability of the porous medium
κ Thermal conductivity
K_T Thermal diffusion ratio,
Kr Chemical reaction
M Magnetic field
N Natural convection
n Order of chemical reaction
Pr Prandtl number
p Pressure
P Porous medium parameter
R Thermal radiation parameter
Re_x Reynolds number
s suction parameter
Sc Schmidt number
Sr Soret number
T Ambient temperature
T_w Temperature at the wall/plate
u_∞ Free steam velocity
u, v x and y velocity components

Greek Symbols

β Casson parameter
β_c Volumetric coefficient of expansion for mass transfer
β_T Volumetric coefficient of expansion for heat transfer
θ Dimensionless temperature
κ Thermal conductivity
λ Mixed convection parameter
μ Dynamic viscosity
ρ Fluid density
τ Cauchy stress tensor
ϕ Dimensionless concentration

Symbol

Δ Change operator
$\Delta\eta$ Mesh spacing

Subscript and superscript

w Surface condition
‘ Differentiation with respect to y
∞ Condition far away from the plate

REFERENCE

AHMAD, K., WAHID, Z. AND HANOUF, Z. (2019). Heat Transfer Analysis for Casson Fluid Flow Over Stretching Sheet with Newtonian Heating and Viscous Dissipation. *Journal of Physics*: Conference. Series 1127(1), 012028. doi:10.1088/1742-6596/1127/1/012028.

ANIMASAUN, I.L. (2015). Effects of Thermophoresis, Variable Viscosity and Thermal Conductivity on Free Convective Heat and Mass Transfer of Non-Darcian MHD Dissipative Casson Fluid Flow with Suction and Nth Order of Chemical Reaction. *Journal of the Nigerian*

Mathematical Society. 34, 11–31. http://dx.doi.org/10.1016/j.jnnms.2014.10.00

BANERJEE, A., MAHATO, S.K., BHATTACHARYYA, K. AND CHAMKHA, A.J. (2021). Divergent Channel Flow of Casson Fluid and Heat Transfer with Suction/Blowing and Viscous Dissipation: Existence of Boundary Layer. *Partial Differential Equations in Applied Mathematics*, 4, 2666-8181. https://doi.org/10.1016/j.padiff.2021.100172

BAOKU, I.G. (2018): Influence of Chemical Reaction, Viscous Dissipation and Joule Heating on MHD Maxwell Fluid Flow with Velocity and Thermal Slip over A Stretching Sheet. *Journal of Advances in Mathematics and Computer Science*, 28, Issue 1, 1 - 20. doi: 10.9734/JAMCS/2018/42481.

BAOKU, I.G. AND FADARE, S.A. (2018): Thermo-Diffusion and Diffusion-Thermo Effects on Mixed Convection Hydromagnetic Flow in A Third Grade Fluid Over A Stretching Surface. *FUDMA Journal of Sciences*, 2, Issue 1, page 23 – 42. http://journal.fudutsinma.edu.ng/index.php/fjs.

BAOKU, I.G. AND FALADE, K. I. (2017): MHD Mixed Convective Flow of a Second Grade Fluid in The Presence of Nonlinearized Thermal Radiation, Thermal-Diffusion and Diffusion-Thermo Effects. *Nigerian Journal of Mathematics and Applications*, 26, page 173-190. http://www.kwsman.com/.

CASTELLANOS, R., SALIH, G., RAIOLA, M., IANIRO, A. AND DISCETTI, S (2023). Heat Transfer Enhancement in Turbulent Boundary Layers with A Pulsed Slot Jetin Crossflow. *Applied Thermal Engineering*. 219, 119595. https://doi.org/10.1016/j.applthermaleng.2022.119595.

HARI, R.K. AND HARSHAD, R.P. (2016). Soret and Heat Generation Effects on MHD Casson Fluid Flow Past an Oscillating Vertical Plate Embedded Through Porous Medium. *Alexandria Engineering Journal*, 55 (3), 2124–2137. http://dx.doi.org/10.1016/j.aej.2016.06.024

HECK A. (2003). Introduction to Maple, 3rd Edition, Springer-Verlag, Germany.

HUSSAIN, M., GHAFFAR, A., ALI, A., SHAHZAD, A., NISAR, K. S., ALHARTHI, M. R. AND JAMSHED, W. (2021). MHD Thermal Boundary Layer Flow of a Casson Fluid over a Penetrable Stretching Wedge in the Existence of Nonlinear Radiation and Convective Boundary Condition. *Alexandria Engineering Journal*, 60(6), 5473–5483. https://doi.org/10.1016/j.aej.2021.03.042.

JALILI, P., AZAR, A.A. JALILI, B. AND GANJI, D.D. (2023). Study of Nonlinear Radiative Heat Transfer with Magnetic Field for Non-Newtonian Casson Fluid Flow in A Porous Medium. *International Journal*, 48, 2211-3797. https://doi.org/10.1016/j.rinp.2023.106371

KAMRAN, A., HUSSAIN, S., SAGHEER, M. AND AKMAL, N. (2017). A Numerical Study of Magnetohydrodynamics Flow in Casson Nanofluid Combined with Joule Heating and Slip Boundary Conditions. *Results Phys.*, **7** 3037–3048. https://doi.org/10.1016/j.rinp.2017.08.004.

KHAN, K.A., BUTT, R.A. AND RAZA, N. (2018). Effects of Heat and Mass Transfer on Unsteady Boundary Layer Flow of a Chemical Reacting Casson Fluid. *Results in Physics*, 8, 610–620. https://doi.org/10.1016/j.rinp.2017.12.080.

MAHANTA, G., DAS, M. AND SHAW, S. (2017). Hydromagnetic Heat and Mass Transfer Flow of a Casson Fluid over an Unsteady Stretching Surface with Convective Boundary Condition. *Journal of Nanofluids*. 6(1). 282–291, doi:10.1166/jon.2017.1311

MAHANTHESH, B., ANIMASAUN, I.L., GORJI, R.M. AND ALARIFI, M.I. (2019). Quadratic Convective Transport of Dusty Casson And Dusty Carreau Fluids Past A Stretched Surface with Nonlinear Thermal Radiation, Convective Condition and Non-Uniform Heat Source/Sink. *Physica A*, 532 378-437. doi.org/10.1016/j.physa.2019.122471

MAJEED, A.H., MAHMOOD, R., SHAHZAD, H., PASHA A.A., RAIZAH, A.Z., HOSHAM, A.H., REDDY, K.S. AND HAFEEZ B.M. (2019). Heat and Mass Transfer Characteristics in MHD Casson Fluid Flow over a Cylinder in A Wavy Channel: Higher-Order FEM computations. *Engineering Journal*, 42, 27-30. http://dx.doi.org/10.1016/j.aej.2016.06.024

MEGAHEDA, A.M. (2015). MHD Viscous Casson fluid flow And Heat Transfer with Second-Order Slip Velocity and Thermal Slip over Permeable Stretching Sheet in The Presence of Internal Heat Generation/Absorption and Thermal Radiation. *Eur. Phys. J. Plus*, 130 (4) 81. DOI 10.1140/epjp/i2015-15081-9.

MIN, S.B., KIM, M.J., HYUNA, K., AHN, W.G. AND KIM, B.C (2023). Thermally Conductive 2D Filler Orientation Control in Polymer Using Thermophoresis. Polymer Testing, 117, 107838. https://doi.org/10.1016/j.polymertesting.2022.107838.

NADEEM, S., ISHTIAQ, B., HAMIDA, MB., ALMUTAIRI, S., GHAZWANI, H.A., ELDIN, S.M

AND AL-SHAFAY, A.S. (2023) Reynolds Nano Fluid Model for Casson Fluid Flow Conveying Exponential Nanoparticles Through A Slandering Sheet. *Scientific Reports*, 13(1) 1953 | https://doi.org/10.1038/s41598-023-28515-1

OBALALU, A.M. (2021) Heat and Mass Transfer in an Unsteady Squeezed Casson Fluid Flow with Novel Thermophysical Properties: Analytical and Numerical Solution. 50(1) 7988–8011. DOI: 10.1002/htj.22263

PAL, D. AND MONDAL, H. (2011). Effects of Soret Dufour, Chemical Reaction and Thermal Radiation on MHD Non-Darcy Unsteady Mixed Convective Heat and Mass Transfer Over a Stretching Sheet. Commun Nonlinear Sci Numer Simulat. 16, 1942–1958.

POPLY, V., SINGH, P. AND YADAV, A.K. (2018). Stability Analysis of MHD Outer Velocity Flow on a Stretching Cylinder. *Alexandria Engineering Journal*, 57(3) 2077–2083. http://dx.doi.org/10.1016/j.aej.2017.05.025

PRAKASH, J., PRASAD, P. D., KUMAR, G. V., KUMAR, K. R. V. M. S. S. AND VURMA, S.V.K (2016). Heat and Mass Transfer Hydromagnetic Radiative Casson Fluid Flow over an Exponentially Stretching Sheet with Heat Source/sink International Journal of Engineering Science Invention 5(7), 12-23. https://www.ijesi.org.

PRAMEELA, M., GANGADHAR, K. AND JITHENDER G. R. (2022). MHD Free Convective Non-Newtonian Casson Fluid Flow Over an Oscillating Vertical Plate. *Partial Differential Equations in Applied Mathematic* 5, 100366. https://doi.org/10.1016/j.padiff.2022.100366.

RAJU, C. S. K., SANDEEP, N., SUGUNAMMA, V., JAYACHANDRA, M. B. AND RAMANA J.R. (2016). Heat and Mass Transfer in Magnetohydrodynamic Casson Fluid over an Exponentially Permeable Stretching Surface. Engineering Science and Technology, an *International Journal*, 19(1) 45-52. doi.org/10.1016/j.jestch.2015.05.010.

REZA-E-RABBI, S.K., ARIFUZZAMA, S.M., SARKAR, T., KHAN, S. M. AND AHMMED, S.F. (2020). Explicit Finite Difference Analysis of An Unsteady MHD Flow of a Chemically Reacting Casson Fluid Past A Stretching Sheet with Brownian Motion and Thermophoresis Effects. *Journal of King Saud University – Science*, 32(1), 690–701. https://doi.org/10.1016/j.jksus.2018.10.017

ROJA, A., GIREESHA, B.J. NAGARAJA, B. (2021). Irreversibility Investigation of Casson Fluid Flow in an Inclined Channel subject to s Darcy-Forchheimer Porous Medium: A Numerical Study. *Applied Mathematics and Mechanics*, 42(1), 95–108. https://doi.org/10.1007/s10483-021-2681-9

SWARNALATHAMMA, B. V., PRAVEEN, D. M. AND KRISHNA, M. V. (2022). Combined Impacts of Radiation Absorption and Chemically Reacting on MHD Free Convective Casson Fluid Flow past an Infinite Vertical Inclined Porous Plate. *Journal of Computational Mathematics and Data Science*, 5, 100069. https://doi.org/10.1016/j.jcmds.2022.100069